

RESEARCH PAPER

Experimental and Numerical Modeling of Seepage in Trapezoidal Channels

Mohamed Kamel Elshaarawy* and Nanes Hassanin Elmasry

Civil Engineering Department, Faculty of Engineering, Horus University-Egypt, New Damietta 34517, Egypt.

*Corresponding author. Email: melshaarawy@horus.edu.eg; mohamed.elshaarawy@eng.psu.edu.eg

(Received 26 November 2024; revised 03 December 2024; accepted 10 December 2024; first published online 31 December 2024)

Abstract

Accurately estimating seepage losses from unlined and lined trapezoidal channels is essential for effective water management, especially in water-scarce regions. This study combined experimental and numerical approaches to evaluate seepage losses, focusing on the influence of channel geometry and liner properties, including hydraulic conductivity (K_L) and thickness (t_L). Firstly, a physical model was constructed, the materials were prepared, and testing procedures were performed to estimate the hydraulic conductivity of the soil and cement mixture. Secondly, five-channel geometries were adjusted in the physical model for unlined and lined experiments. Finally, the Slide2 model results were compared with the experimental data. Results revealed that the Slide2 numerical model accurately estimated seepage losses from unlined and lined trapezoidal channels compared to the physical model with a high determination coefficient (R^2) of 0.99 and 0.99 and low root-mean-squared-error (RMSE) values of 2.85 and 0.03 $\text{cm}^3 \text{s}^{-1}$, respectively. For unlined channels, the seepage losses increased with larger bed width-to-water depth ratios due to the extended wetted perimeter. For lined channels, lining was ineffective when K_L exceeded 0.01, while a 0.05 increase in t_L reduced seepage losses by 15%. Furthermore, design charts and equations were developed to estimate the seepage losses from unlined and lined channels considering channel dimensions, liner hydraulic conductivity, and thickness.

Keywords: Seepage losses; Lining; Trapezoidal channel; Physical model; Slide2 model; Regression; SEEP/W.

1. Introduction

Seepage serves as the principal mechanism of water loss in irrigation canals [1]. Seepage is defined as the infiltration of water through the canal bed and sides, where it permeates vertically and migrates laterally through the surrounding soil, ultimately diminishing the efficiency of water conveyance by reducing the volume available for irrigation. This reduction can hinder timely and equitable water distribution essential for meeting crop demands [2], [3]. Furthermore, seepage can elevate unconfined groundwater tables, causing groundwater to move upward via capillary action, leading to soil surface saturation. This can cause waterlogging and salt accumulation in the root zone, which can harm crop yields and reduce productivity [4]. In regions with natural vegetation or fallow land, shallow groundwater levels promote non-beneficial water use through evaporation and transpiration by weeds and phreatophytes [5]. Additionally, seepage influences subsurface return flows into canals, further compromising the efficiency of water conveyance systems, highlighting the importance of managing seepage in water resource strategies [6].

Various methodologies exist for quantifying canal seepage, including field techniques such as localized point measurements, ponding tests, and inflow–outflow methods; however, these approaches often encounter practical challenges that limit their widespread application [7]. Empirical formulas and analytical models based on factors like canal discharge, flow velocity, and soil hydraulic properties are commonly used, though numerical modeling has gained favor due to its efficiency and reduced data requirements [8]. When configured with accurate boundary conditions, numerical models provide a reliable method for estimating seepage losses. Prior research has explored seepage using diverse approaches, including direct measurements, empirical formulations, and analytical techniques [9], [10], [11]. Nonetheless, lining irrigation canals has emerged as an effective approach to mitigating seepage, employing liners such as compacted soil, soil–cement mixtures, asphaltic concrete, flexible membranes, and conventional concrete, which act as barriers to water loss [12], [13]. Canal lining not only reduces seepage but also enhances flow, lowers maintenance costs, suppresses weed growth, and mitigates waterlogging in adjacent agricultural areas [14], [15], [16], [17].

Researchers assessed the water losses in both lined and unlined channels in a specific region of the Indus Basin in Pakistan, finding that lining reduced water losses by 22.5% [18]. Similarly, researchers compared water losses in four lined watercourses, observing a reduction from 66% in unlined waterways to an average of 43.5% in lined ones [19]. The transportation efficiency in the lined sections ranged from 83% to 90%, while unlined sections showed efficiencies between 36% and 69%. Researchers studied various watercourse improvement alternatives, calculating average water loss rates of 1.91, 3.08, and 2.51 liters per second per 100-meter length for different watercourse types [20]. Their findings demonstrated that lining was more effective than earthen renovation and cleaning for achieving long-term water savings. Another research quantified transportation losses from lined and unlined sections of a canal irrigation network, determining that the effectiveness and total losses from lined and unlined canal sections, as well as unlined field channels, were 75%, 52%, and 35%, respectively, with corresponding water losses of 0.184, 0.61, and 0.183 Mm³ [21].

Analysis used a water balance approach to assess seepage losses along a canal of significant length, with results indicating substantial uncertainty in the probability distributions of losses, ranging from a slight gain to approximately 0.110 m³/s per hectare of the canal's wetted perimeter, or 0.043–0.95 m/day [22]. The impact of canal lining on groundwater recharge was investigated in the lower Bhavan basin, revealing that unlined canals recharge groundwater approximately 20% more effectively than lined canals [23]. Researchers studied conveyance losses in tertiary channel systems across South Asia, showing that in Pakistan, lined watercourses account for 43.5% of water losses, while unlined watercourses account for 66% [24]. In contrast, in India, the losses from lined watercourses range from 11% to 25%, with unlined systems losing between 20% and 25%. Researchers explored the optimal design of concrete canal sections to minimize water losses and earthworks costs, using MATLAB for optimization [25]. The results, presented as dimensionless graphs, provided simplified solutions for the optimal design of canal dimensions at the lowest cost per meter.

Further studies on watercourse efficiency have demonstrated the benefits of canal lining in improving conveyance. Researchers investigated water conveyance efficiency and cropping intensity in three lined watercourses in the Jamrao canal command, finding that 30% lining in the initial portion of watercourses resulted in a 6.5 ha–m water savings, allowing for an additional 7 ha of land to be cultivated [26]. The cropping intensity increased by 29% during the Rabi season and 12% during the Kharif season. Research studied the enhancement of irrigation water conveyance efficiency under Egyptian conditions, comparing earthen canals, lined canals, and buried pipes made of PVC [27]. Their results showed conveyance efficiencies of 65%, 92.2%, and 98.7% in winter and 59.6%, 87.1%, and 89.7% in summer for earthen canals, lined canals, and buried pipes, respectively. The lined canals and buried pipes significantly reduced conveyance losses by 68.1% and 96.3% in summer, and 77.7% and 96.3% in winter compared to earthen canals. Researchers conducted a comparative study of

lining techniques in Bahawalnagar district, Pakistan, where the irrigation water losses for precast concrete parabolic-lined watercourses ranged from 35% to 52%, while those for rectangular lining ranged from 64% to 68% [28]. This study also compared watercourses with different lining forms, including rectangular brick masonry and circular precast parabolic pieces.

Advanced modeling techniques have enhanced seepage analysis in irrigation canals, with hybrid approaches like SEEP/W combined with Evolutionary Polynomial Regression (EPR) yielding more accurate estimates of seepage loss in Isfahan and Qazvin canals in Iran [29]. Beyond modeling, both geometric and hydraulic factors significantly affect seepage rates. For example, higher hydraulic conductivity, larger freeboard, steeper slopes, and greater channel height all increase seepage in triangular channels, underscoring the importance of both liner and canal design considerations [30]. Further research on trapezoidal, rectangular, and triangular canals using SEEP/W emphasized the wetted perimeter as a primary factor in seepage, with side slope having a lesser effect [31]. Liners themselves continue to be a focal point in seepage reduction efforts. Comparisons between canals lined with random rubble (RR) masonry and low-density polyethylene (LDPE) showed that LDPE achieved lower seepage losses (2%) compared to RR (8%) [32].

Such findings reinforce the importance of selecting appropriate liners based on the specific seepage reduction goals and the conditions in which canals operate. Unlined canals also provide critical insights, as they enable comparisons with lined counterparts. In these unlined channels, the SEEP/W model was found to yield more accurate seepage loss estimates than empirical methods, which often resulted in substantial errors [33]. Research into compacted earth linings has shown that highly compacted soils can reduce seepage discharge by up to 99.8%, suggesting that preparation of the canal surface itself can play a significant role in seepage control [34]. Further research highlighted the hydraulic conductivity of the lining as the most influential factor on seepage rates, independent of groundwater table depth or canal berm width, emphasizing that liner selection and its hydraulic properties are key to achieving long-term seepage reduction [35]. Moreover, studies in Egypt on the El-Sont Canal using the Slide2 and FLOW-3D models demonstrated that cement concrete (CC) and LDPE linings could reduce seepage losses by 97% and increase canal discharge by an average of 150% [36].

Despite extensive research on seepage losses in irrigation canals and the effectiveness of various lining materials, significant gaps remain in understanding the combined impact of geometric parameters and lining properties on seepage in trapezoidal channels under diverse hydraulic conditions. Most existing studies focus either on specific canal shapes or rely heavily on numerical models without comprehensive validation against experimental results. Furthermore, while numerical models have demonstrated accuracy, limited research has integrated physical modeling with advanced numerical simulations, such as the Slide2 model, to evaluate seepage losses in a systematic and comparative manner. Additionally, the long-term effectiveness and interaction of various geometric factors, such as channel bed width, side slopes, and liner thickness, remain underexplored.

This study addresses critical gaps in understanding seepage losses from unlined and lined trapezoidal channels by combining experimental measurements with numerical simulations using the Slide2 model. Thus, the main objectives are (1) To experimentally measure seepage losses from unlined and lined trapezoidal channels using a physical model; (2) To validate the experimental results through numerical simulations using the Slide2 model; (3) To evaluate the effect of various geometric parameters on seepage losses; (4) To assess the impact of different types of canal lining on seepage reduction; (5) To provide practical recommendations for optimizing canal design and lining selection in sustainable irrigation practices.

2. Materials and Methods

The methodological approach can be described in Figure 1. In this study, a physical model and Slide2 numerical model were used to estimate seepage losses from unlined and lined trapezoidal channels.

Ten experimental tests were conducted using the physical model by varying channel bed width to water depth ratio before and after the lining process. Subsequently, the Slide2 model was calibrated by two experimental tests and validated by the other three experiments. The agreement between estimated seepage losses from both models was judged using several statistical parameters based on correlation and error measurements for the calibration and validation processes. Moreover, a seepage analysis was performed to investigate the effect of geometric parameters and lining on seepage losses from unlined and lined trapezoidal channels.

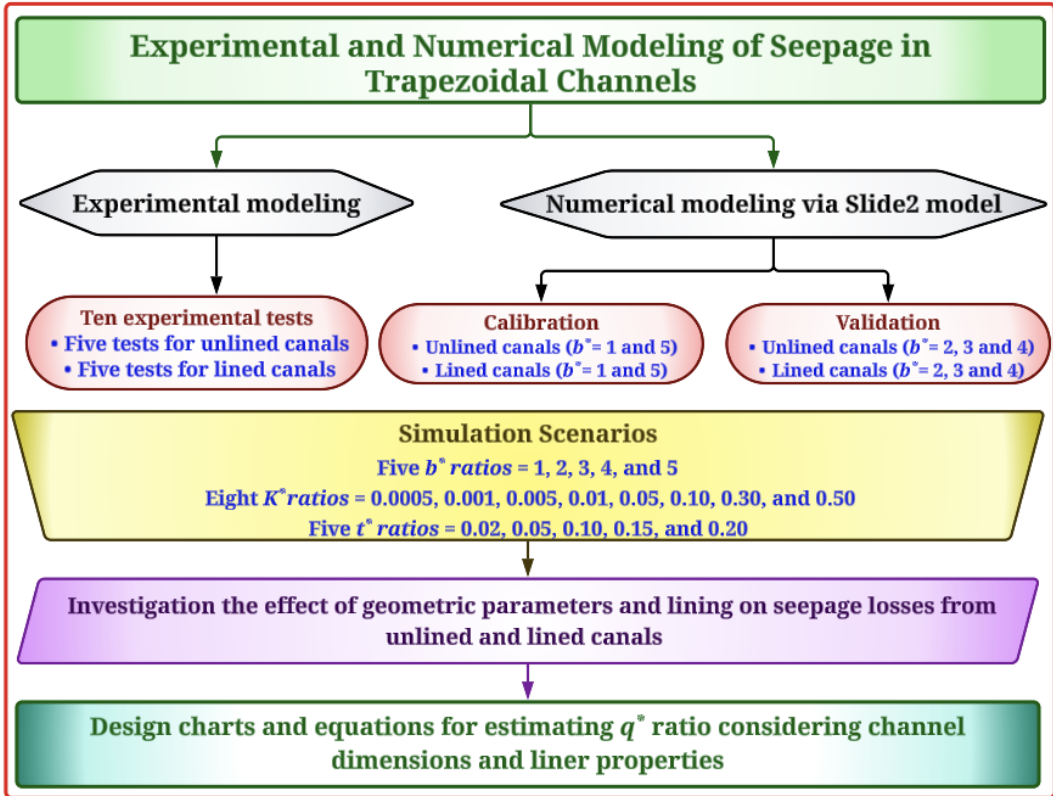


Figure 1: Methodological flowchart adopted in this study.

2.1 Effective Parameters

This study investigates the geometric and hydraulic parameters that influence seepage losses in trapezoidal channels. Seepage losses, denoted as q_{s0} are analyzed in relation to several key factors: the soil hydraulic conductivity (K), channel bed width (b), water depth (γ), liner thickness (t_L), and liner hydraulic conductivity (K_L). Using dimensional analysis, the relationship between these parameters is expressed mathematically. Eq. (1) presents this as a general functional relationship.

$$f(q_s, b, \gamma, K_L, K, t_L) = 0 \tag{1}$$

Where f is a functional symbol. By applying Buckingham's π theorem, the functional relationship is refined, yielding a dimensionless form shown in Eq. (2).

$$\left(\frac{q_s}{K \cdot \gamma}, \frac{b}{\gamma}, \frac{K_L}{K}, \frac{t_L}{\gamma} \right) = 0 \tag{2}$$

This equation simplifies the analysis by consolidating variables into dimensionless terms, making it easier to study the interactions between the parameters. Further, Eq. (3) rewrites the π terms into compact forms.

$$(q^*, b^*, K^*, t^*) = 0 \rightarrow q^* = f(b^*, K^*, t^*) \tag{3}$$

This indicates that seepage losses, represented in dimensionless form (q^*), depend on three other dimensionless groups (b^*, K^*, t^*).

2.2 Experimental Modeling

2.2.1 Description of physical model

A physical model was constructed within rectangular tanks made of 1 cm thick securit glass, with dimensions of 100 cm in length, 50 cm in width, and 100 cm in height. The tank bottom was designed with eight 1/2-inch diameter slots connected to a drainage system comprising two 3/4-inch diameter pipelines, each equipped with four drainage slots. Fig. 2a shows the longitudinal layout of the physical model, including the tank dimensions and drainage configuration, while Fig. 2 b illustrates the transverse view, and Fig. 2c shows an image for the constructed physical model. The construction process began with placing a sand barrier at the tank bottom, followed by the addition and compaction of soil in 20 cm layers. The channel side slopes were shaped and compacted to conform to a 2H : 1 V gradient. Laboratory tests determined the soil hydraulic conductivity to be 0.052 cms^{-1} , ensuring the model's suitability for accurately simulating hydraulic conditions.

2.2.2 Experimental tests

The experiments were divided into two groups; an unlined channel (Fig. 3a) and a lined channel (Fig. 3b). Ten experimental tests were conducted. Firstly, the channel section shape was created with a constant water level of 20 cm by varying channel bed width to water depth ratio (i.e., $b^* = 1, 2, 3, 4,$ and 5). The channel was filled with water to the desired level and maintained at that level to achieve soil saturation with a constant rate of seepage. The seepage losses were calculated using the volumetric method given by Moghazi [37] as follows:

$$Q_s = \frac{WL(\gamma_1 - \gamma_2)}{PT} \tag{4}$$

Where W is the average top channel width (cm), L is the channel length (cm), γ_1 is the initial water depth (cm), P is the average wetted perimeter (cm), γ_2 is the water depth after time T (cm), Q_s is the seepage losses per unit channel length ($\text{cm}^3 \text{ s}^{-1}$).

For the lining experiments, the channel was coated with a cement mixture of 2 cm thickness, covering both the bed and inner side slope of the channel. The cement mixture was composed of sand, cement, and water in a 4:2:1 ratio, respectively. To assess the hydraulic conductivity of the cement mixture, a sorptivity test was performed [38]. This test measures the rate of water absorption by monitoring the increase in sample mass over time, with only one surface exposed to water entry through capillary suction [39]. Fig. 4 illustrates the cement mixture disc sealing and the sorptivity test setup. The cumulative volume of absorbed water per unit surface area (I) was calculated using Eq. (5), as shown below:

$$I = \frac{M}{\rho A} \tag{5}$$

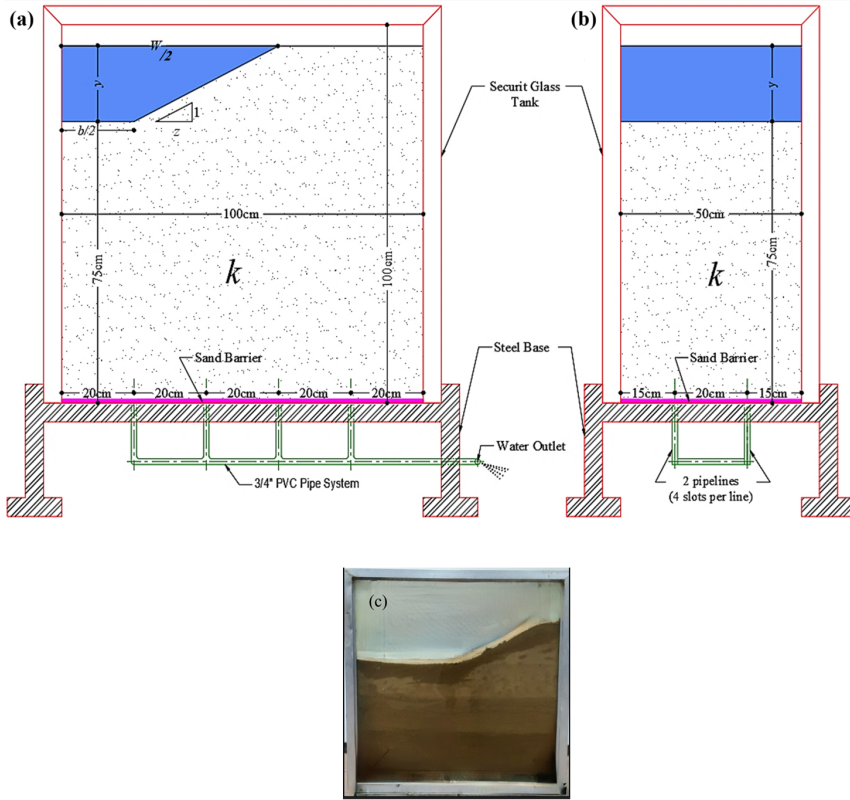


Figure 2: Schematic of the constructed physical model: (a) longitudinal direction, (b) transverse direction, (c) image of an experiment.

Where ρ is the density of water gm/cm^3 , A is the exposed area of the bottom surface (cm^2), and M is the specimen mass variation at a given time (gm). Consequently, the liner hydraulic conductivity (K_L) was calculated from Eq. (6) as $1.044 \times 10^{-6} \text{ cm s}^{-1}$.

$$K_L = \frac{I}{T} \tag{6}$$

2.3 Numerical modeling

2.3.1 Model description

In this study, the Slide2 model was employed to estimate seepage losses from both unlined and lined trapezoidal channels. Additionally, the model was used to investigate the combined effect of lining and channel geometry on seepage losses. The Slide2 model utilizes a built-in finite element method for groundwater seepage analysis, allowing it to simulate water flow through a porous medium [40]. Eq. (7) is the governing equation in the Slide2 model and was given by Mahmud [41].

$$K_x \frac{\partial^2 H}{\partial x^2} + K_y \frac{\partial^2 H}{\partial y^2} = 0 \tag{7}$$

Where H is the total head, K_x and K_y are the soil hydraulic conductivity in the x and y directions, respectively.

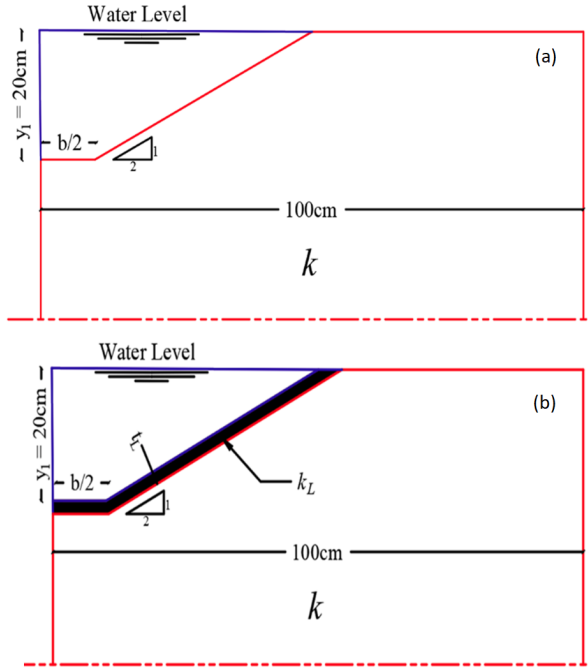


Figure 3: Trapezoidal channel: (a) unlined and (b) lined sections.

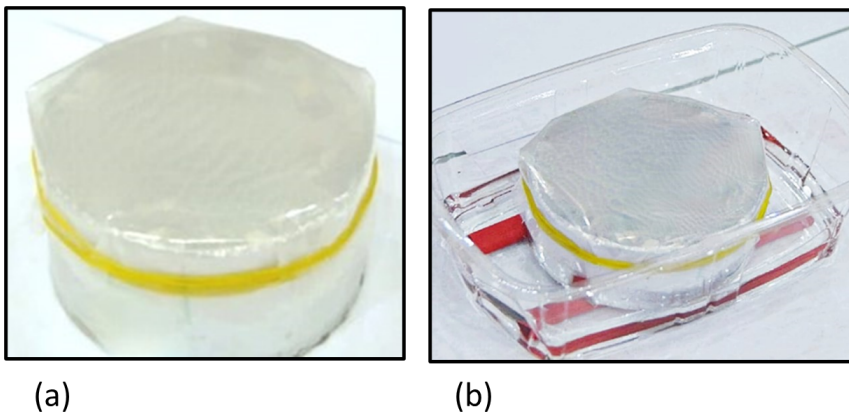


Figure 4: Cement mixture disc: (a) sealing process and (b) sorptivity test.

2.4 Model setup

Seepage flow was assumed to move vertically downwards, and no influence of groundwater on seepage was considered during the simulation [42]. Mesh refinement was used during discretizing the simulation domain to capture any slight change in fluxes within the simulation domain [43]. Three thousand mesh elements of 3-noded triangles element were used to build the simulation domain. Firstly, the material properties and unlined channel dimensions were entered. Subsequently, the liner hydraulic conductivity and thickness were defined in the model. Then, the boundary conditions were entered as total head and exit seepage face at the channel perimeter and domain

bottom, respectively. After that, the discharge section was defined to estimate the seepage losses. Finally, the seepage analysis was interpreted, and the seepage losses at the selected discharge section were obtained. Fig. 5 shows effective parameters affecting seepage losses showing the simulation domain and the imposed boundary conditions.

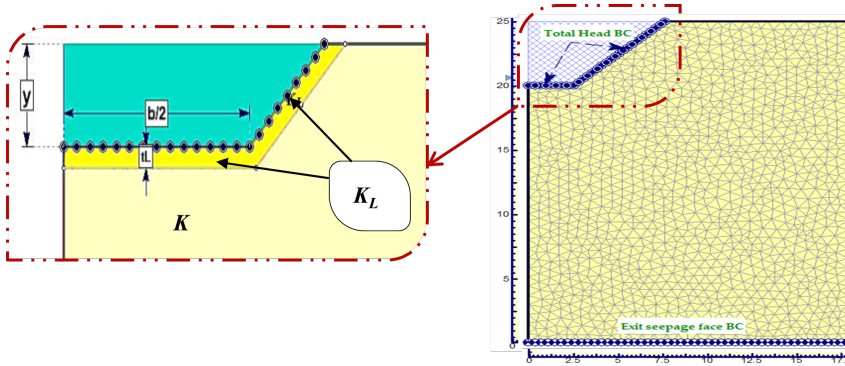


Figure 5: Schematic of the channel geometry along with the simulation domain and imposed boundary conditions.

2.4.1 Simulation scenarios

After the validation process, the combined effects of lining and channel geometry on seepage losses were investigated to develop design charts and equations for estimating seepage losses in both unlined and lined trapezoidal channels. A total of 225 simulation scenarios were performed using the Slide2 model, including 200 scenarios for lined channels, with variations in b^* (1, 2, 3, 4, 5), K^* (0.0005, 0.001, 0.005, 0.01, 0.05, 0.10, 0.30, 0.50), and t^* (0.01, 0.05, 0.10, 0.15, 0.20). These parameter ranges were selected to encompass most real-world canal geometries and typical values for liner hydraulic conductivity and thickness. The remaining 25 scenarios were dedicated to calibration and validation for unlined channels as the reference case. Boundary conditions were defined similarly to the calibration process to ensure consistency.

2.4.2 Evaluation Criteria

The Slide2 model was calibrated using two experimental tests, with channel bed width to water depth ratios (b^*) of 1 and 5, representing the smallest and largest geometries within the study range. This selection ensured that the model captured seepage behaviors across the entire spectrum of channel geometries, from narrow to wide configurations. The hydraulic conductivities (K and K_L) derived from laboratory tests for sand and cement mixtures were incorporated into the model. The statistical parameters used for calibration and their corresponding equations are presented in Table 1. Model validation was performed by comparing seepage losses predicted by the Slide2 model with those estimated from three additional experimental tests, where the channel bed width to water depth ratios were varied ($b^* = 2, 3, 4$). The performance of the Slide2 model was evaluated using a comprehensive set of statistical criteria [44]. The correlation-based evaluation included the correlation coefficient (r), index of agreement (d), and Nash-Sutcliffe Efficiency (NSE). The error-based evaluation involved root mean square error (RMSE), mean absolute error (MAE), mean absolute percentage error (MAPE), and R-squared (R^2). These metrics assessed the agreement between seepage losses predicted by the Slide2 model and the experimental results, with n representing the dataset size, x is the seepage losses from the physical model, y is the seepage losses from the Slide2 model, and \bar{x} is the mean seepage losses estimated by the Slide2 model.

3. Results and Discussion

3.1 Slide2 Model Validation

Table 2 presents the estimated seepage losses obtained from the physical model (Q_s Exp) and the Slide2 model (Q_s Num) during the calibration and validation processes for both unlined and lined channels. The results indicate that the Slide2 model predictions closely align with the experimental results, demonstrating high accuracy and reliability. For the calibration process, at a channel bed width-to-water depth ratio (b^*) of 1, the unlined channel exhibited seepage losses (Q_s Exp) of $102.64 \text{ cm}^3 \text{ s}^{-1}$ and (Q_s Num) of $109.05 \text{ cm}^3 \text{ s}^{-1}$. Similarly, for $b^* = 5$, the experimental and numerical seepage losses were 178.75 and $171.54 \text{ cm}^3 \text{ s}^{-1}$, respectively. The lined channel, however, exhibited significantly reduced seepage losses, with values ranging from $1.07 \text{ cm}^3 \text{ s}^{-1}$ to $1.87 \text{ cm}^3 \text{ s}^{-1}$, confirming the efficacy of the lining process in mitigating seepage. For the validation process, the unlined channel seepage losses for $b^* = 2, 3$, and 4 ranged between $121.72 \text{ cm}^3 \text{ s}^{-1}$ and $159.77 \text{ cm}^3 \text{ s}^{-1}$, while the Slide2 model predicted seepage losses within a similar range of $122.32 \text{ cm}^3 \text{ s}^{-1}$ to $154.87 \text{ cm}^3 \text{ s}^{-1}$. For the lined channel, seepage losses remained minimal, with values between $1.27 \text{ cm}^3 \text{ s}^{-1}$ and $1.67 \text{ cm}^3 \text{ s}^{-1}$, which closely matched the Slide2 model predictions.

Table 1: Statistical parameters for the performance assessment.

Set	Statistical parameter	Symbol	Equation
Based on the Correlation	Correlation coefficient [45]	r	$\frac{n[\sum_{i=1}^n x_i y_i] - (\sum_{i=1}^n x_i)(\sum_{i=1}^n y_i)}{\sqrt{[n \sum_{i=1}^n (x_i^2) - (\sum_{i=1}^n x_i)^2][n \sum_{i=1}^n (y_i^2) - (\sum_{i=1}^n y_i)^2]}}$
	Index of agreement [46]	d	$1 - \frac{\sum_{i=1}^n (x_i - y_i)^2}{\sum_{i=1}^n (x_i - \bar{x} + y_i - \bar{y})^2}$
	Nash Sutcliffe efficiency [47]	NSE	$1 - \frac{\sum_{i=1}^n (x_i - y_i)^2}{\sum_{i=1}^n (x_i - \bar{x})^2}$
Based on Errors	Root mean square error [48]	RMSE	$\sqrt{\frac{\sum_{i=1}^n (x_i - y_i)^2}{n}}$
	Mean absolute error [49]	MAE	$\frac{\sum_{i=1}^n x_i - y_i }{n}$
	Mean absolute percentage error [50]	MAPE	$\frac{100 \times \sum_{i=1}^n \left \frac{x_i - y_i}{x_i} \right }{n}$
	R-squared [51], [52]	R^2	$\left[\frac{n[\sum_{i=1}^n x_i y_i] - (\sum_{i=1}^n x_i)(\sum_{i=1}^n y_i)}{\sqrt{[n \sum_{i=1}^n x_i^2 - (\sum_{i=1}^n x_i)^2][n \sum_{i=1}^n y_i^2 - (\sum_{i=1}^n y_i)^2]}} \right]^2$

Table 2: Results of seepage losses during calibration and validation for unlined and lined trapezoidal channels.

Process	b^*	Unlined Channel		Lined Channel	
		Q_{sExp} ($\text{cm}^3 \text{ s}^{-1}$)	Q_{sNum} ($\text{cm}^3 \text{ s}^{-1}$)	Q_{sExp} ($\text{cm}^3 \text{ s}^{-1}$)	Q_{sNum} ($\text{cm}^3 \text{ s}^{-1}$)
Calibration	1	102.64	109.05	1.07	1.15
	5	178.75	171.54	1.87	1.81
Validation	2	121.72	122.32	1.27	1.29
	3	140.76	141.04	1.47	1.49
	4	159.77	154.87	1.67	1.63

The strong agreement between Q_{sExp} and Q_{sNum} for both calibration and validation cases underscores the Slide2 model’s capability to accurately simulate seepage losses in both unlined

and lined trapezoidal channels. The differences between experimental and numerical results were marginal, with deviations well within acceptable ranges for predictive models. These discrepancies may be attributed to minor experimental uncertainties or model assumptions, such as uniform soil properties and boundary conditions. The results also emphasize the critical impact of channel lining in reducing seepage losses. The lined scenarios showed an average reduction in seepage losses of over 99% compared to the unlined cases, highlighting the importance of implementing channel lining as a water conservation strategy.

The statistical analysis results presented in Table 3 further validate the reliability and accuracy of the Slide2 model in estimating seepage losses for both unlined and lined trapezoidal channels. For the calibration process, the unlined channel exhibited excellent performance metrics, with correlation-based parameters such as r , d , and NSE all achieving values of 0.99 or 0.97. Error-based parameters, including RMSE ($6.82 \text{ cm}^3 \text{ s}^{-1}$), MAE ($6.81 \text{ cm}^3 \text{ s}^{-1}$), and MAPE (5.14%), further confirmed the model's high precision. For the lined channel, similar accuracy was observed, with r , d , and NSE all at 0.99 or 0.97, and significantly lower RMSE ($0.07 \text{ cm}^3 \text{ s}^{-1}$), MAE ($0.07 \text{ cm}^3 \text{ s}^{-1}$), and MAPE (5.20%). The validation process yielded comparable results, demonstrating the robustness of the Slide2 model across different scenarios. For unlined channels, the model achieved r , d , and NSE values of 0.99 or 0.97, along with low RMSE ($2.85 \text{ cm}^3 \text{ s}^{-1}$), MAE ($1.93 \text{ cm}^3 \text{ s}^{-1}$), and MAPE (1.25%). The lined channel again exhibited superior performance, with r , d , and NSE values of 0.99 or 0.98, and minimal error values, including RMSE ($0.03 \text{ cm}^3 \text{ s}^{-1}$), MAE ($0.02 \text{ cm}^3 \text{ s}^{-1}$), and MAPE (1.65%).

Table 3: Estimated performance indices for the calibration and validation processes of the Slide2 model.

Process	b^*	Correlation-based parameters			Error-based parameters			
		r	d	NSE	RMSE ($\text{cm}^3 \text{ s}^{-1}$)	MAE ($\text{cm}^3 \text{ s}^{-1}$)	MAPE (%)	R^2
Calibration	Unlined	0.99	0.99	0.97	6.82	6.81	5.14	0.99
	Lined	0.99	0.99	0.97	0.07	0.07	5.20	0.99
Validation	Unlined	0.99	0.99	0.97	2.85	1.93	1.25	0.99
	Lined	0.99	0.99	0.98	0.03	0.02	1.65	0.99

The Slide2 model demonstrated exceptional performance across varying channel geometries and lining conditions, showcasing its robustness and adaptability for diverse hydraulic scenarios. High correlation values and consistently low error metrics in both calibration and validation processes validate its reliability in replicating physical seepage loss measurements. The model's ability to accurately capture the effects of channel geometry and the significant reduction in seepage losses due to lining further highlights its utility. Overall, the Slide2 model is a dependable tool for predicting seepage losses and optimizing trapezoidal channel designs in a variety of hydraulic conditions.

3.2 Effect of investigated parameters on seepage losses in the unlined channels

The analysis of seepage losses in unlined channels demonstrated a clear positive correlation between the channel bed width-to-water depth ratio (b^*) and the seepage losses (q^*). As b^* increased from 1 to 5, the seepage losses estimated by the Slide2 model rose from 7.6 to 12.8, with an average increment of approximately 14% per unit increase in b^* ratio. This trend is scientifically attributed to several factors. First, as b^* increases, the wetted perimeter of the channel expands, providing a larger surface area for seepage to occur. The longer infiltration pathway directly contributes to greater water losses through the channel bed and side slopes. Additionally, a wider channel bed increases the horizontal hydraulic gradient, allowing water to seep more laterally through the surrounding soil, further exacerbating seepage losses. The expanded contact surface area between the water and the channel bed enhances the soil-water interaction, intensifying infiltration rates, particularly in

permeable soils. Moreover, higher b^* ratios typically correspond to shallower water depths, which increase the surface-to-volume ratio and magnify the impact of seepage relative to the available water volume. These combined factors explain the observed trend and highlight the critical role of channel geometry in influencing seepage dynamics. The derived linear regression equation ($q^* = 1.30b^* + 6.314$) with R^2 of 0.99, further validates the reliability of the Slide2 model in predicting seepage behavior in unlined channels.

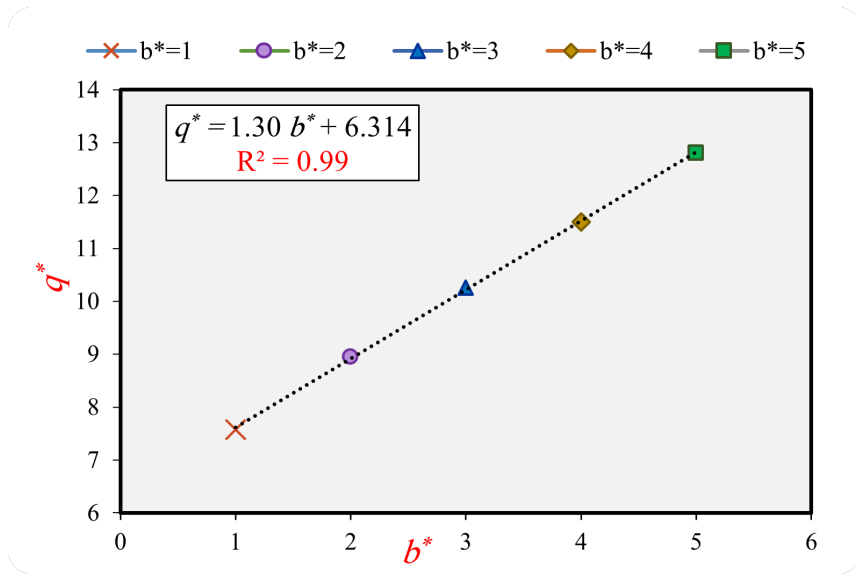


Figure 6: Relationship between q^* and b^* for unlined channels.

3.3 Effect of investigated parameters on seepage losses in the lined channels

The results in Figs. 7 and 8 illustrate the influence of key parameters, including liner hydraulic conductivity (K^*) and liner thickness (t^*), on seepage losses (q^*) in lined trapezoidal channels. The figures provide detailed trends for different values of channel bed width-to-water depth ratios (b^*), highlighting the significant role of these parameters in controlling seepage.

3.3.1 Liner hydraulic conductivity (K_L)

The results in Fig. 7 demonstrate a strong relationship between K^* and q^* , with higher values of K^* leading to a significant increase in seepage losses for all investigated values of t^* . This behavior can be attributed to the increased permeability of the liner material, which allows water to infiltrate more readily through the liner, thereby reducing its effectiveness as a barrier. For example, at $t^* = 0.02$, seepage losses remain minimal for low K^* values (e.g., $K^* < 0.01$) but rise steeply as K^* exceeds this threshold, reaching the highest losses at $K^* = 0.50$. A similar trend is observed at higher t^* values, although the absolute seepage losses decrease with increasing t^* , reflecting the combined effect of hydraulic conductivity and liner thickness on seepage control.

The effect of b^* is also evident in these results. For all values of t^* , seepage losses are consistently higher at larger b^* ratios, as wider channels have larger wetted perimeters, increasing the infiltration surface area and promoting higher water losses. This demonstrates that the channel geometry interacts with liner hydraulic conductivity to influence seepage rates. The results emphasize the need for selecting low-permeability liner materials, especially for wider channels with higher b^* ratios, to minimize seepage losses. The findings also highlight that, for very high K^* values, the performance

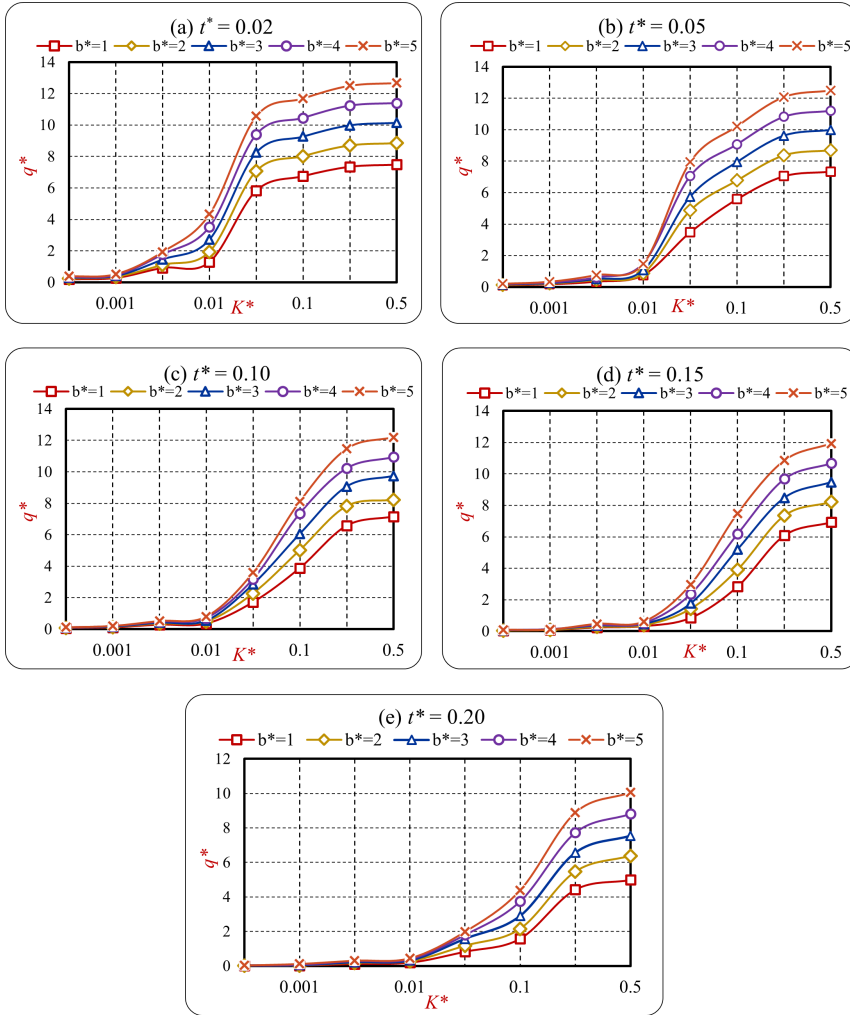


Figure 7: Estimated q^* values under different K^* and b^* ratios at t^* of (a) 0.02, (b) 0.05, (c) 0.10, (d) 0.15 and (e) 0.20.

of the liner deteriorates significantly, making it critical to control the quality and permeability of the liner material during design and construction.

Thus, this analysis underscores the importance of accurately determining liner hydraulic conductivity before implementation. Even small deviations in K^* can result in significant changes in seepage rates, particularly in channels with large b^* ratios. Moreover, the sharp rise in seepage losses with increasing K^* demonstrates that maintaining a low liner permeability is not only essential for reducing water loss but also for ensuring the long-term sustainability of the canal system.

3.3.2 Liner thickness (t_l)

The results in Fig. 8 show that increasing liner thickness (t^*) has a pronounced effect in reducing q^* across all b^* ratios and K^* values. This reduction can be explained by the longer infiltration pathway created by thicker liners, which increases the resistance to water flow and reduces the rate of seepage. For instance, at $K^* = 0.01$, seepage losses drop sharply as t^* increases from 0.02 to 0.10, with the rate

of reduction becoming less pronounced for t^* values beyond 0.10 . This trend reflects the diminishing returns of adding liner thickness, where the marginal improvement in seepage reduction decreases with increased t^* . The influence of b^* is also significant in these results. Channels with larger b^* ratios consistently exhibit higher seepage losses at all t^* values, which can be attributed to the increased wetted perimeter in wider channels. This larger surface area provides more opportunities for water to infiltrate through the liner, even as t^* increases. However, the relative reduction in seepage losses with increasing t^* is consistent across all b^* ratios, indicating that the effect of liner thickness is robust regardless of channel geometry.

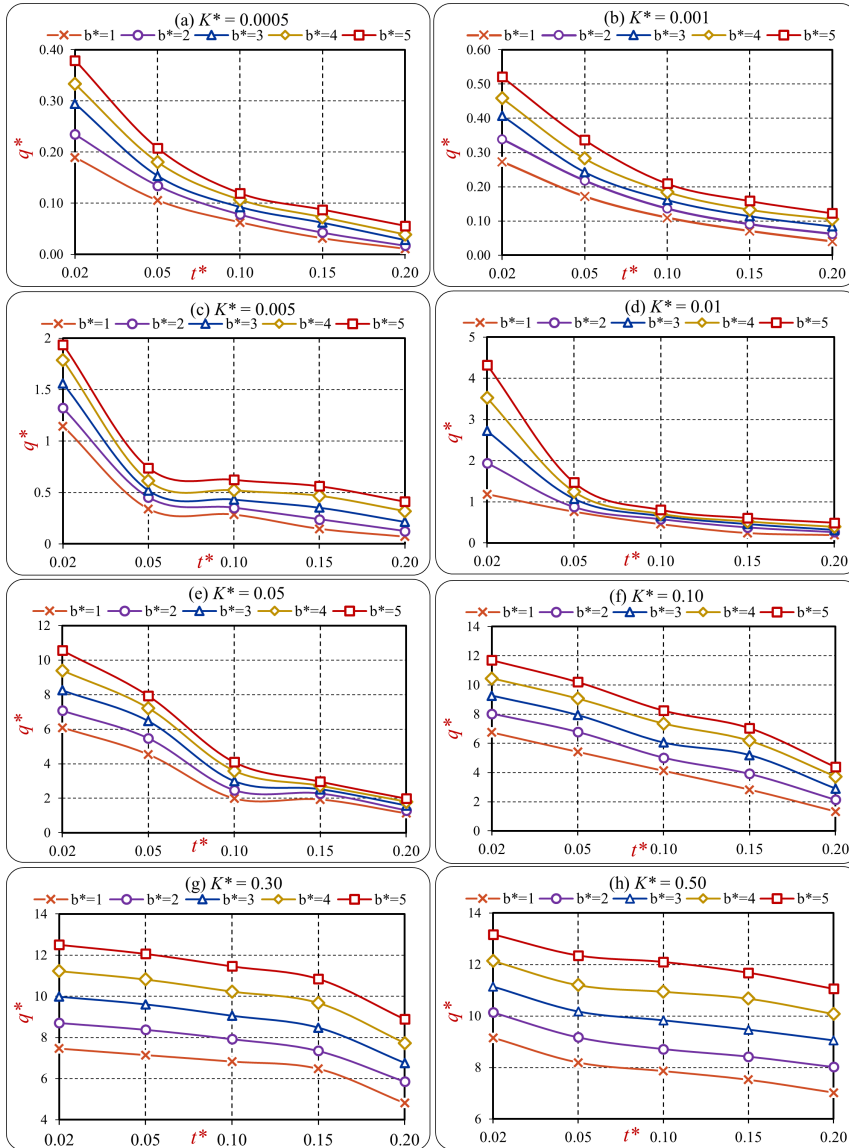


Figure 8: Estimated q^* values under different t^* and b^* ratios at K^* of (a) 0.0005, (b) 0.001, (c) 0.005, (d) 0.01, (e) 0.05, (f) 0.10, (g) 0.30 and (h) 0.50.

Thus, the results highlight the critical role of liner thickness in seepage control. Thicker liners

create a longer flow path, reducing the hydraulic gradient and thereby lowering the seepage rate. However, the diminishing returns observed at higher t^* values suggest that there is an optimal thickness beyond which additional material may not provide significant benefits. This has important implications for cost-effectiveness, as excessively thick liners may not justify the added expense. These findings also have practical implications for the design of lined trapezoidal channels. While increasing t^* is an effective strategy for reducing seepage losses, its effectiveness is influenced by other parameters such as K^* and b^* . For channels with high K^* values, thicker liners are essential to compensate for the increased permeability, whereas in channels with low K^* values, a moderate liner thickness may suffice. Similarly, wider channels with larger b^* ratios require thicker liners to offset the increased seepage potential due to their larger wetted perimeters.

3.3.3 Predictive equation for q^*

A predictive equation was developed to quantify the relationship between seepage losses and the key influencing parameters. The equation is derived from the nonlinear regression analysis using Statistical Package for the Social Sciences (SPSS) software. It can be expressed as follows in Eq. (8).

$$q^* = 6.144 (b^*)^{0.33} \times (K^*)^{0.42} \times (t^*)^{-0.188} \tag{8}$$

Fig. 9 shows a scatter plot between actual and predicted q^* values obtained from the Slide2 models and Eq. (8), respectively. The plot displays the degree of alignment between predicted and actual values, with closer clustering around the equality line indicating better predictive performance. Dashed lines represent $\pm 20\%$ deviation from the equality line, serving as a reference for model accuracy. Predicted values by Eq. (8) show strong alignment with actual values, as indicated by high R^2 values of 0.908 and low RMSE.

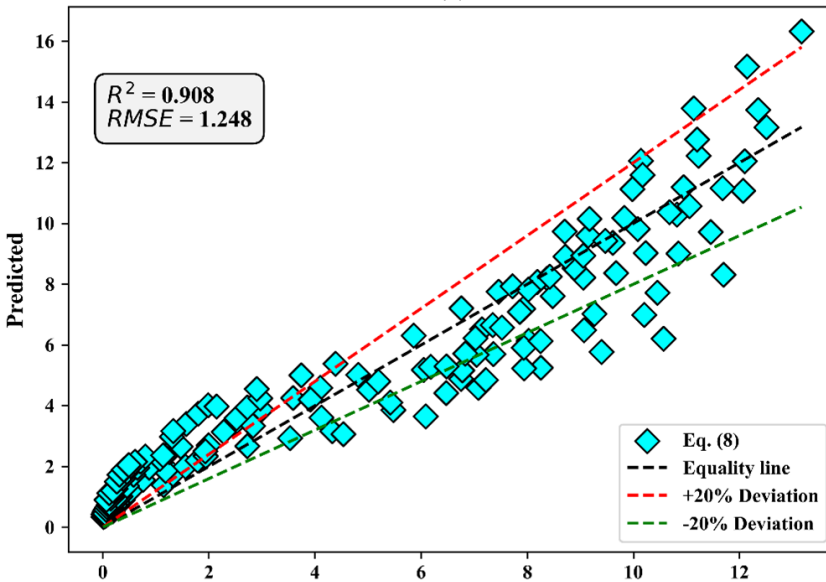


Figure 9: Scatter plot indicating the actual versus predicted q^* values.

The positive exponents of b^* and K^* indicate that seepage losses increase with larger channel widths and higher liner hydraulic conductivities, as these factors enhance the wetted perimeter and permeability of the liner, respectively. Conversely, the negative exponent of t^* demonstrates that increasing the liner thickness effectively reduces seepage losses by extending the infiltration pathway

and increasing resistance to water flow. This predictive equation offers a comprehensive and reliable tool for estimating seepage losses in trapezoidal channels, providing insights that are critical for the design and optimization of canal systems. Its application facilitates the evaluation of various design scenarios, enabling effective decision-making for sustainable water resource management and seepage control strategies.

4. Conclusion

This study evaluated seepage losses from unlined and lined trapezoidal channels using experimental and numerical approaches. The Slide2 model was validated against experimental results, showing high accuracy and reliability in predicting seepage losses across different geometric and hydraulic conditions. The results demonstrated that channel geometry and liner properties significantly influence seepage losses. For unlined channels, seepage increased with larger bed width-to-water depth ratios due to the extended wetted perimeter and infiltration pathway. For lined channels, the effectiveness of the liner was highly dependent on its hydraulic conductivity and thickness. Low liner permeability and increased thickness significantly reduced seepage losses, highlighting the importance of optimizing liner materials and dimensions for effective water conservation. A predictive equation was developed, providing a robust tool to estimate seepage losses based on the key parameters of channel geometry and liner properties. With a correlation coefficient (R^2) of 0.908, this equation offers valuable insights for the design and optimization of trapezoidal channels under diverse conditions. The findings underscore the importance of incorporating both geometric and material considerations in seepage control strategies to enhance water resource sustainability.

The study's strengths include the comprehensive validation of the Slide2 model, which ensures the reliability of the simulation results. Additionally, the combination of experimental data and numerical simulations provides a more holistic understanding of seepage behavior under various conditions. The developed predictive equation offers a practical tool for engineers, providing a means to optimize canal designs for better water conservation in real-world applications. The study's focus on both liner material properties and channel geometry also contributes to a more nuanced approach to seepage control, offering insights that can be directly applied to improving the efficiency of irrigation systems.

Despite the strengths of this study, several limitations should be noted. The experimental setup relied on a controlled environment, which may not fully replicate the complexities of field conditions, such as soil heterogeneity, climate variability, and long-term liner performance. Additionally, the model assumes uniform soil properties and steady-state seepage, which may not reflect transient conditions observed in real-world scenarios. These simplifications could influence the generalizability of the findings to diverse field settings.

Future studies should validate the Slide2 model and predictive equation in field-scale conditions, accounting for soil heterogeneity, climate variability, and transient flow scenarios. Long-term performance and durability of various liner materials should be investigated, including their resistance to degradation. Additionally, integrating advanced modeling techniques or machine learning could enhance prediction accuracy and adaptability for complex hydraulic systems.

Funding: This research received no external funding.

Disclosure statement: The author reported no potential conflict of interest.

Data availability statement: All data underlying the results are available as part of the article, and no additional source data is required.

References

- [1] A. A. R. Lund, T. K. Gates, and J. Scalia, "Characterization and control of irrigation canal seepage losses: A review and perspective focused on field data," *Agric. Water Manag.*, vol. 289, p. 108516, 2023, doi: 10.1016/j.agwat.2023.108516.

- [2] M. K. Elshaarawy, M. Elkiki, T. Selim, and M. G. Eltarabily, "Hydraulic comparison of different types of lining for irrigation canals using computational fluid dynamic models." Civil Engineering Department, Faculty of Engineering, Port Said University ..., 2024.
- [3] M. G. Eltarabily, H. F. Abd-Elhamid, M. Zeleňáková, M. K. Elshaarawy, M. Elkiki, and T. Selim, "Predicting seepage losses from lined irrigation canals using machine learning models," *Front. Water*, vol. 5, 2023, doi: 10.3389/frwa.2023.1287357.
- [4] M. G. Eltarabily, T. Selim, M. K. Elshaarawy, and M. H. Mourad, "Numerical and experimental modeling of geotextile soil reinforcement for optimizing settlement and stability of loaded slopes of irrigation canals," *Environ. Earth Sci.*, vol. 83, no. 8, 2024, doi: 10.1007/s12665-024-11560-y.
- [5] M. K. Elshaarawy, N. H. Elmasry, T. Selim, M. Elkiki, and M. G. Eltarabily, "Determining Seepage Loss Predictions in Lined Canals Through Optimizing Advanced Gradient Boosting Techniques," *Water Conserv. Sci. Eng.*, vol. 9, no. 2, 2024, doi: 10.1007/s41101-024-00306-3.
- [6] S. L. Atmapoojya, R. N. Ingle, A. R. Kacimov, P. K. Swamee, G. C. Mishra, and B. R. Chahar, "Design of Minimum Seepage Loss Canal Sections," *J. Irrig. Drain. Eng.*, vol. 127, no. 3, pp. 189–192, 2001, doi: 10.1061/(asce)0733-9437(2001)127:3(189).
- [7] R. P. Vishnoi and R. Saxena, "Determination of seepage losses in unlined channels," *Int. J. Comput. Appl.*, vol. 975, p. 8887, 2014.
- [8] S. S. Christian, "Seepage through Canals' – A Review," *Int. J. Res. Appl. Sci. Eng. Technol.*, vol. 6, no. 4, pp. 865–867, 2018, doi: 10.22214/ijraset.2018.4146.
- [9] H. F. Isleem, M. K. Elshaarawy, and A. K. Hamed, "Analysis of Flow Dynamics and Energy Dissipation in Piano Key and Labyrinth Weirs Using Computational Fluid Dynamics," *Computational Fluid Dynamics – Analysis, Simulations, and Applications [Working Title]*. IntechOpen, 2024. doi: 10.5772/intechopen.1006332.
- [10] Y. M. Ghazaw, "Design and analysis of a canal section for minimum water loss," *Alexandria Eng. J.*, vol. 50, no. 4, pp. 337–344, 2011, doi: 10.1016/j.aej.2011.12.002.
- [11] A. Carabineanu, "Free-Boundary Seepage from Asymmetric Soil Channels," *Int. J. Math. Math. Sci.*, vol. 2012, pp. 1–14, 2012, doi: 10.1155/2012/962963.
- [12] I. Abd-Elaty, L. Pugliese, K. M. Bali, M. E. Grismer, and M. G. Eltarabily, "Modelling the impact of lining and covering irrigation canals on underlying groundwater stores in the Nile Delta, Egypt," *Hydrol. Process.*, vol. 36, no. 1, 2022, doi: 10.1002/hyp.14466.
- [13] K. Ding and L. Gao, "Development in canal lining technology in China," *Irrig. Drain.*, vol. 69, no. S2, pp. 36–40, 2020, doi: 10.1002/ird.2438.
- [14] F. B. Sarand and M. Hajjalilue-Bonab, "Effect of Unsaturated Expansive Soils on Canal Linings: A Case Study on the Tabriz Plain Canal, Iran," *Irrig. Drain.*, vol. 66, no. 3, pp. 396–410, 2017, doi: 10.1002/ird.2113.
- [15] H. Plusquellec, "OVERESTIMATION OF BENEFITS OF CANAL IRRIGATION PROJECTS: DECLINE OF PERFORMANCE OVER TIME CAUSED BY DETERIORATION OF CONCRETE CANAL LINING," *Irrig. Drain.*, vol. 68, no. 3, pp. 383–388, 2019, doi: 10.1002/ird.2341.
- [16] S. Abd-Elziz, M. Zeleňáková, B. Kršák, and H. F. Abd-Elhamid, "Spatial and Temporal Effects of Irrigation Canals Rehabilitation on the Land and Crop Yields, a Case Study: The Nile Delta, Egypt," *Water*, vol. 14, no. 5, p. 808, 2022, doi: 10.3390/w14050808.
- [17] M. Mutema and K. Dhavu, "Review of factors affecting canal water losses based on a meta-analysis of worldwide data," *Irrig. Drain.*, vol. 71, no. 3, pp. 559–573, 2022, doi: 10.1002/ird.2689.
- [18] M. Ashour, T. sayed, and A. Atef, "Water-Saving from Rehabilitation of Irrigation Canals Case Study: El-Sont Canal, Assiut Governorate," *Aswan Univ. J. Environ. Stud.*, vol. 0, no. 0, p. 0, 2021, doi: 10.21608/aujes.2021.89249.1034.
- [19] F. Javaid, M. Arshad, M. Azam, A. Shabbir, and A. Shakoor, "Performance assessment of

- lined watercourses in district Jhang,” *Pak. J. Agri. Sci.*, vol. 49, no. 1, pp. 79–83, 2012.
- [20] Z. A. Chatha, M. Arshad, A. Bakhsh, and A. Shakoor, “Design and cost analysis of water-course lining for sustainable water saving,” *J. Agric. Res.*, vol. 52, no. 4, 2014.
- [21] P. B. Jadhav, R. T. Thokal, Ms. Mane, H. N. Bhange, and S. R. Kale, “Conveyance efficiency improvement through canal lining and yield increment by adopting drip irrigation in command area,” *Int. J. Innov. Res. Sci. Eng. Technol.*, vol. 3, no. 4, pp. 120–129, 2014.
- [22] C. A. Martin and T. K. Gates, “Uncertainty of canal seepage losses estimated using flowing water balance with acoustic Doppler devices,” *J. Hydrol.*, vol. 517, pp. 746–761, 2014, doi: 10.1016/j.jhydrol.2014.05.074.
- [23] M. Gad, H. M. Abdelhaleem, and W. OAS, “Forecasting the seepage loss for lined and un-lined canals using artificial neural network and gene expression programming,” *Geomatics, Nat. Hazards Risk*, vol. 14, no. 1, p. 2221775, 2023.
- [24] T. Sultan, A. Latif, A. S. Shakir, K. Kheder, and M. U. Rashid, “Comparison of water conveyance losses in unlined and lined watercourses in developing countries,” *Univ. Eng. Technol. Taxila. Tech. J.*, vol. 19, no. 2, p. 23, 2014.
- [25] M. M. Rezapour Tabari, S. Tavakoli, and M. Mazak Mari, “Optimal Design of Concrete Canal Section for Minimizing Costs of Water Loss, Lining and Earthworks,” *Water Resour. Manag.*, vol. 28, no. 10, pp. 3019–3034, 2014, doi: 10.1007/s11269-014-0652-9.
- [26] M. A. Mangrio et al., “ECONOMIC FEASIBILITY OF WATERCOURSES LINING IN SINDH PAKISTAN,” *Sci. Int.*, vol. 27, no. 2, 2015.
- [27] E. A. M. Osman, G. A. Bakeer, M. E. Abuarab, and M. T. Eltantawy, “IMPROVING IRRIGATION WATER CONVEYANCE AND DISTRIBUTION EFFICIENCY USING LINED CANALS AND BURIED PIPES UNDER EGYPTIAN CONDITION,” *Misr J. Agric. Eng.*, vol. 33, no. 4, pp. 1399–1420, 2016, doi: 10.21608/mjae.2016.97611.
- [28] M. Zubair, A. Nasir, S. Z. H. Shah, and M. Arshad, “Comparative study of lining watercourses techniques in Bahawalnagar district in Pakistan,” *Intl. J. Engg. Appl. Sci. Technol.*, vol. 1, no. 12, pp. 73–80, 2016.
- [29] E. Aghvami, A. Abbaspour, M. A. Ghorbani, and F. Salmasi, “Estimation of channels seepage using SEEP/W and evolutionary polynomial regression (EPR) modeling (Case study: Qazvin and Isfahan channels),” *J. Civ. Eng. Urban.*, vol. 3, no. 4, pp. 211–215, 2013.
- [30] A. Abdul Jabbar Jamel, “Analysis and Estimation of Downward Seepage from Lining and Unlining Triangular Open Channel,” *Eng. Technol. J.*, vol. 34, no. 2, pp. 406–419, 2016, doi: 10.30684/etj.34.2a.18.
- [31] F. Salmasi and J. Abraham, “Predicting seepage from unlined earthen channels using the finite element method and multi variable nonlinear regression,” *Agric. Water Manag.*, vol. 234, p. 106148, 2020, doi: 10.1016/j.agwat.2020.106148.
- [32] S. M. V Sharief and M. Zakwan, “Comparative analysis of seepage loss through different canal linings,” *Int. J. Hydrol. Sci. Technol.*, vol. 1, no. 1, p. 1, 2021, doi: 10.1504/ijhst.2021.10037172.
- [33] R. Hosseinzadeh Asl, F. Salmasi, and H. Arvanaghi, “Numerical investigation on geometric configurations affecting seepage from unlined earthen channels and the comparison with field measurements,” *Eng. Appl. Comput. Fluid Mech.*, vol. 14, no. 1, pp. 236–253, 2020, doi: 10.1080/19942060.2019.1706639.
- [34] D. A. El-Molla and M. A. El-Molla, “Reducing the conveyance losses in trapezoidal canals using compacted earth lining,” *Ain Shams Eng. J.*, vol. 12, no. 3, pp. 2453–2463, 2021, doi: 10.1016/j.asej.2021.01.018.
- [35] M. G. Eltarabily, M. K. Elshaarawy, M. Elkiki, and T. Selim, “Modeling surface water and groundwater interactions for seepage losses estimation from unlined and lined canals,” *Water Sci.*, vol. 37, no. 1, pp. 315–328, 2023, doi: 10.1080/23570008.2023.2248734.
- [36] M. G. Eltarabily, M. K. Elshaarawy, M. Elkiki, and T. Selim, “Computational fluid dy-

- namics and artificial neural networks for modelling lined irrigation canals with low-density polyethylene and cement concrete liners,” *Irrig. Drain.*, vol. 73, no. 3, pp. 910–927, 2023, doi: 10.1002/ird.2911.
- [37] H. E. M. Moghazi and E.-S. Ismail, “A study of losses from field channels under arid region conditions,” *Irrig. Sci.*, vol. 17, no. 3, pp. 105–110, 1997, doi: 10.1007/s002710050028.
- [38] A. C1585-13, “Standard test method for measurement of rate of absorption of water by hydraulic-cement concretes,” *ASTM Int.*, vol. 41, no. 147, pp. 1–6, 2013.
- [39] M. M. Alsaadawi, M. Amin, and A. M. Tahwia, “Thermal, mechanical and microstructural properties of sustainable concrete incorporating Phase change materials,” *Constr. Build. Mater.*, vol. 356, p. 129300, 2022, doi: 10.1016/j.conbuildmat.2022.129300.
- [40] Rocscience, “Groundwater module in slide 2D finite element program for groundwater analysis verification manual.” Rocscience Inc Toronto, 2011.
- [41] M. Mahmud, “Spreadsheet Solutions To Laplace’s Equation: Seepage And Flow Net,” *J. Teknol.*, pp. 53–67, 1996, doi: 10.11113/jt.v25.1008.
- [42] V. V Vedernikov, “Theory of seepage and its application in irrigation and drainage,” *Gosstrojizdat*, Moscow, 1939.
- [43] M. K. Elshaarawy and A. K. Hamed, “Stacked ensemble model for optimized prediction of triangular side orifice discharge coefficient,” *Eng. Optim.*, pp. 1–31, 2024.
- [44] M. Kamel Elshaarawy and M. G. Eltarabily, “Machine learning models for predicting water quality index: optimization and performance analysis for El Moghra, Egypt,” *Water Supply*, vol. 24, no. 9, pp. 3269–3294, 2024.
- [45] H. F. Isleem *et al.*, “Numerical and machine learning modeling of GFRP confined concrete-steel hollow elliptical columns,” *Sci. Rep.*, vol. 14, no. 1, p. 18647, 2024.
- [46] M. A. Elazab *et al.*, “Exploring the potential of conical solar stills: Design optimization and enhanced performance overview,” *Desalin. Water Treat.*, p. 100642, 2024.
- [47] M. K. Elshaarawy, M. M. Alsaadawi, and A. K. Hamed, “Machine learning and interactive GUI for concrete compressive strength prediction,” *Sci. Rep.*, vol. 14, no. 1, p. 16694, 2024.
- [48] W. Tian, H. F. Isleem, A. K. Hamed, and M. K. Elshaarawy, “Enhancing discharge prediction over Type-A piano key weirs: An innovative machine learning approach,” *Flow Meas. Instrum.*, vol. 100, p. 102732, 2024.
- [49] T. Selim, M. K. Elshaarawy, M. Elkiki, and M. G. Eltarabily, “Estimating seepage losses from lined irrigation canals using nonlinear regression and artificial neural network models,” *Appl. Water Sci.*, vol. 14, no. 5, 2024, doi: 10.1007/s13201-024-02142-1.
- [50] M. K. Elshaarawy and A. K. Hamed, “Predicting discharge coefficient of triangular side orifice using ANN and GEP models,” *Water Sci.*, vol. 38, no. 1, pp. 1–20, 2024.
- [51] M. G. Eltarabily and M. K. Elshaarawy, “Risk Assessment of Potential Groundwater Contamination by Agricultural Drainage Water in the Central Valley Watershed, California, USA,” in *Groundwater Quality and Geochemistry in Arid and Semi-Arid Regions*, Springer, 2023, pp. 37–76.
- [52] M. Elshaarawy, A. K. Hamed, and S. Hamed, “Regression-based models for predicting discharge coefficient of triangular side orifice,” *J. Eng. Res.*, vol. 7, no. 5, pp. 224–231, 2023.